Ziegler, M., Rajabi, M., Heidbach, O., Hersir, G. P., Ágústsson, K., Árnadóttir, S., Zang, A. (2016): The stress pattern of Iceland. - *Tectonophysics*, *674*, pp. 101—113.
DOI: http://doi.org/10.1016/j.tecto.2016.02.008

The Stress Pattern of Iceland

Moritz Ziegler[a,b,*], Mojtaba Rajabi[c], Oliver Heidbach[a], Gylfi Páll Hersir[d], Kristján Ágústsson[d], Sigurveig Árnadóttir[d], Arno Zang[a,b]

[a] *Helmholtz Centre Potsdam, German Research Centre for Geosciences, Telegrafenberg, 14473 Potsdam, Germany*
[b] *University of Potsdam, Institute of Earth and Environmental Science, Karl-Liebknecht-Str. 24-25, 14476 Potsdam-Golm, Germany*
[c] *Australian School of Petroleum, The University of Adelaide, Adelaide, SA 5005, Australia*
[d] *Iceland GeoSurvey (ÍSOR), Grensásvegur 9, 108 Reykjavík, Iceland*

Abstract

Iceland is located on the Mid-Atlantic Ridge which is the plate boundary between the Eurasian and the North American plates. It is one of the few places on earth where an active spreading centre is located onshore but the stress pattern has not been extensively investigated so far. In this paper we present a comprehensive compilation of the orientation of maximum horizontal stress (S_{Hmax}). In particular we interpret borehole breakouts and drilling induced fractures from borehole image logs in 57 geothermal wells onshore Iceland. The borehole results are combined with other stress indicators including earthquake focal mechanism solutions, geological information and overcoring measurements resulting in a dataset with 495 data records for the S_{Hmax} orientation. The reliability of each indicator is assessed according to the quality criteria of the World Stress Map project.

The majority of S_{Hmax} orientation data records in Iceland is derived from earthquake focal mechanism solutions (35%) and geological fault slip inversions (26%). 20% of the data are borehole related stress indicators. In addition minor shares of S_{Hmax} orientations are compiled, amongst others, from focal mechanism inversions and the alignment of fissure eruptions. The results show that the S_{Hmax} orientations derived from different depths and stress indicators are consistent with each other.

The resulting pattern of the present-day stress in Iceland has four distinct subsets of S_{Hmax} orientations. The S_{Hmax} orientation is parallel to the rift axes in the vicinity of the active spreading regions. It changes from NE-SW in the South to approximately N-S in central Iceland and NNW-SSE in the North. In the Westfjords which is located far away from the ridge the regional S_{Hmax} rotates and is parallel to the plate motion.

Journal: Tectonophysics, 674, 101–113, DOI: 10.1016/j.tecto.2016.02.008
Received 13 August 2015, Revised 29 January 2016, Accepted 2 February 2016, Available online 12 February 2016

Keywords: Iceland, Stress Field, Stress Pattern, Borehole image log

1. Introduction

The regional stress pattern along divergent plate boundaries has not been studied extensively yet due to the inaccessibility of submerged Mid Oceanic Ridges. Few and scattered earthquake focal mechanism solutions are the only sources of stress orientation in these areas in the World Stress Map (WSM) database (Heidbach et al., 2008, 2010). These indicators generally show a ridge parallel maximum horizontal stress (S_{Hmax}) orientation (Zoback et al., 1989; Zoback, 1992). In intraplate regions the orientation of S_{Hmax} is often parallel to the absolute plate motion in a first order approximation and therefore generally normal to the ridges and subduction zones (e.g. Richardson, 1992; Müller et al., 1992; Grünthal and Stromeyer, 1992; Zoback, 1992; Zoback et al., 1989). A systematic rotation of S_{Hmax} from ridge parallel to ridge normal has

*Corresponding author:
Email address: mziegler@gfz-potsdam.de (Moritz Ziegler)

been observed close to ridges in the Indian Ocean (Wiens and Stein, 1984) and at Mid Oceanic Ridges in general (Sykes, 1967; Sykes and Sbar, 1974).

Iceland is one of the few places on the Earth with an onshore divergent plate boundary (e.g. Ward, 1971; Sæmundsson, 1979; Einarsson, 1991, 2008; Bird, 2003). It is in a unique geological and tectonic setting, where an oceanic ridge (the Mid-Atlantic Ridge) traverses a (purported) mantle plume (e.g. Lawver and Müller, 1994; Wolfe et al., 1997; Allen et al., 2002). The rift zones in and around Iceland are dominated by various volcanic systems of different extents and activities (Thordarson and Larsen, 2007; Jóhannesson and Sæmundsson, 1998). Induced by the hotspot the plumbing of the volcanic systems is extended compared to a usual divergent plate boundary (Allen et al., 2002). As the plate boundary crosses the hotspot, it breaks up into a complex series of segments. Purely divergent segments are the Northern Volcanic Zone (NVZ) in North Iceland, and the sub-parallel Western and Eastern Volcanic Zones (WVZ, EVZ) in South Iceland which are generally assumed to be the expression of a ridge jump (Sæmundsson, 1979; Einarsson, 1991, 2008). In the South, the South Iceland Seismic Zone (SISZ) is the connecting segment between the Reykjanes peninsula and the Eastern Volcanic Zone (Sæmundsson, 1974, 1979; Einarsson, 1991; Stefánsson et al., 2008). In the North the Tjörnes Fracture Zone (TFZ) connects the NVZ to the southern end of the submarine Kolbeinsey Ridge (Sæmundsson, 1974, 1979; Einarsson, 1991; Stefánsson et al., 2008). The WVZ and NVZ are joined by a transverse E-W zone across central Iceland. Outside of the immediate plate boundary, volcanism occurs in the South Iceland Volcanic Zone, the Snæfellsnes Volcanic Zone and the Öræfajökull Volcanic Zone (e.g. Jakobsson, 1979; Sæmundsson, 1978, 1986).

This volcano-tectonic setting has received a particular attention in the first compilation of the present-day crustal stress by Hast (1969). Since then, several researchers investigated the state of stress in different parts of Iceland. An extensive campaign of in-situ stress measurements from shallow overcorings was carried out by Schäfer and Keil (1979). Haimson and Rummel (1982) conducted hydro-fracturing experiments in six onshore boreholes. Furthermore, extensive field campaigns to collect geological fault slip data provide information on the current and palaeo-stress field in Iceland as well as its temporal evolution (Gudmundsson et al., 1996; Bergerat and Angelier, 1998; Garcia and Dhont, 2005; Angelier et al., 2008; Plateaux et al., 2012). In total, the compilation of stress data records in the World Stress Map (WSM) database 2008 resulted in 38 data records of the contemporary S_{Hmax} orientation and the stress regime (9 focal mechanism solutions, 5 hydro-fracturing orientations, and 24 overcoring measurements, Heidbach et al., 2008, 2010). However, this small data set is not sufficient to reveal the presumably high variability of the stress field pattern of Iceland. This is especially important since Iceland's peculiar location causes extensive interactions between tectonic and volcanic processes which influence the local stress field (e.g. Sæmundsson, 1979; Gudmundsson, 2006; Andrew and Gudmundsson, 2008).

In this paper we present a new comprehensive compilation of the contemporary S_{Hmax} orientation for Iceland with 495 data records (Fig. 1). In particular, we analysed 37 km of borehole acoustic image logs from 57 geothermal wells to interpret present-day stress indicators, i.e. borehole breakouts (BOs) and drilling induced fractures (DIFs). Furthermore, we revised the 38 data records from the WSM 2008 and conducted an extensive literature study to compile published focal mechanism solutions and geological stress indicators, e.g. fault slip inversions or the alignment of volcanic vents and fissures. All data records are quality ranked according to the WSM quality ranking system (Zoback, 1992; Sperner et al., 2003; Heidbach et al., 2010). We identify the regional pattern of the S_{Hmax} orientation by four different stress provinces with different mean S_{Hmax} orientations on Iceland.

2. Stress data compilation

The first comprehensive compilation of the contemporary S_{Hmax} orientation was made by Sbar and Sykes (1973) who mapped the stress pattern in North America. This effort was later institutionalised by Zoback et al. (1989) in the framework of the WSM project (e.g. Müller et al., 1992; Heidbach et al., 2010). In the literature there are several methods to determine the orientation of S_{Hmax} in a rock volume (Ljunggren et al., 2003; Zoback et al., 1989; Zang and Stephansson, 2010). However, these different methods may result in different orientations due to the depth of the phenomena, different reliability, or superposition of different forces at different scales (Heidbach et al., 2007). Hence,

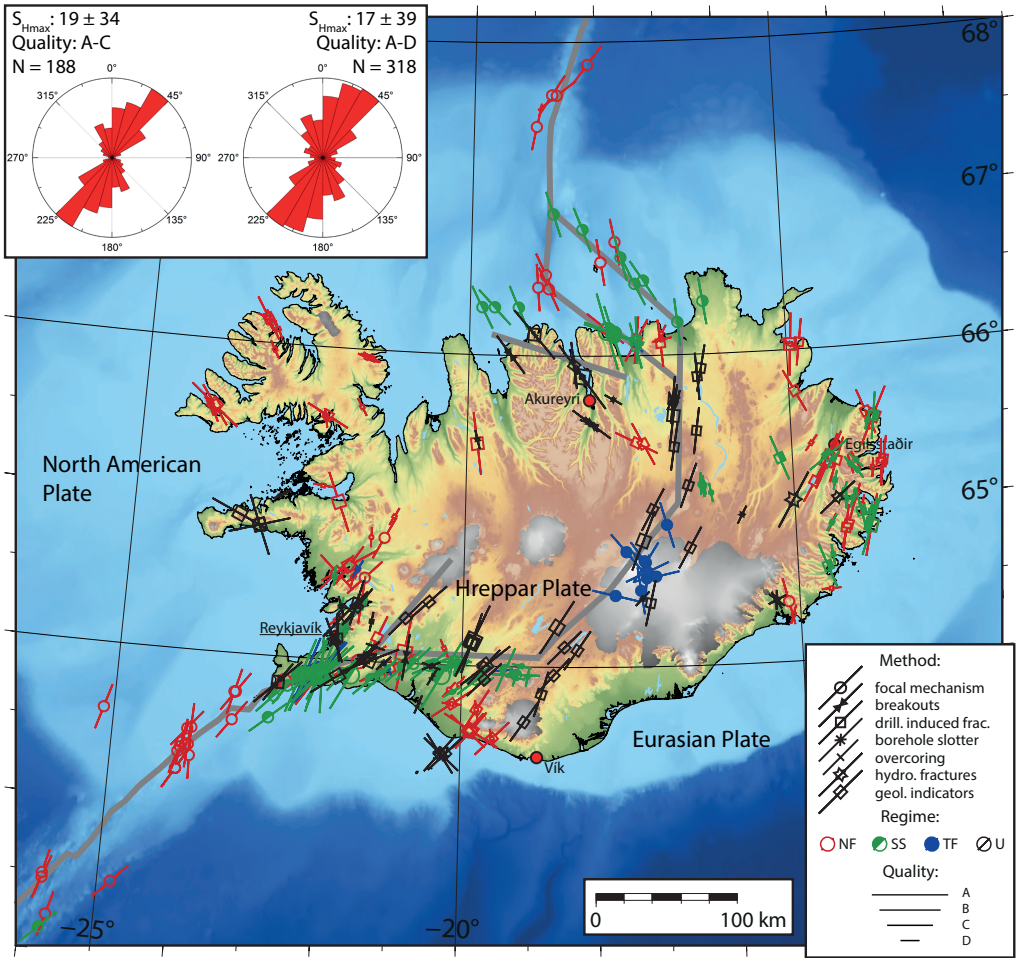

Figure 1: The first comprehensive stress map of Iceland with 318 data records with A-D quality according to the World Stress Map quality criteria (Sperner et al., 2003; Heidbach et al., 2010). Lines represent the orientation of maximum horizontal stress S_{Hmax} with the length proportional to quality. The symbols in the middle of the lines display the method used for stress determination. The colour coding is according to the stress regime with red indicating normal faulting, green indicating strike slip faulting, blue indicating thrust/reverse faulting, and black for unknown regimes. The plate boundaries according to Bird (2003) and Einarsson (2008) are indicated in grey. Two rose diagrams display the unweighted frequency distribution of the A-C and A-D quality data respectively. Mean S_{Hmax} orientations and their standard deviations are calculated with the circular statistics of bi-polar data (Mardia, 1972).

comparison between the S_{Hmax} from different indicators have received a particular attention to establish a quality ranking scheme for the WSM database (Zoback and Zoback, 1991; Zoback, 1992; Zoback et al., 1989; Sperner et al., 2003; Heidbach et al., 2010). Following this scheme each data record is assigned a quality from A (reliability of orientation ± 15°), B (± 15-20°), C (± 20-25°), D (± 25-40°) up to E (> ± 40°) (Heidbach et al., 2010). A detailed description of the WSM quality ranking scheme for individual stress indicators can be found in Zoback (1992), Sperner et al. (2003), and Heidbach et al. (2010).

Our stress data compilation extends from 62° to 68° northern latitude and from -11° to -26° longitude. The image log data from the 57 geothermal wells resulted in 36 new A-D stress data records. In addition, we estimated 17 S_{Hmax} orientations from crater rows of fissure eruptions of different volcanic systems. Furthermore, an extensive literature review resulted in 374 new stress data records which are mainly from focal mechanism solutions of earthquakes. These new data records are from different earthquake catalogues such as the Global CMT (Ekström et al., 2012; Dziewonski et al., 1981), Geofon Potsdam (Centre, 1993) and Zurich Moment Tensors. Furthermore data records were included from published papers by Angelier et al. (2004); Batir (2011); Bergerat et al. (1990); Bergerat and Angelier (1998); Bergerat et al. (1998); Bergerat and Plateaux (2012); Bjarnason and Einarsson (1991); Einarsson (1979, 1987); Forslund and Gudmundsson (1991); Garcia et al. (2002); Garcia (2003); Green et al. (2014); Gudmundsson et al. (1992); Gudmundsson (1995); Gudmundsson et al. (1996); Jakobsson (1979); Jefferis and Voight (1981); Hagos et al. (2008); Haimson and Voight (1977); Keiding et al. (2009); Khodayar and Franzson (2007); Kristjánsdóttir (2013); Lund and Slunga (1999); Lund and Bödvarsson (2002); Nakamura (1977); Plateaux et al. (2014); Rögnvaldsson and Slunga (1994); Roth et al. (2000); Schäfer and Keil (1979); Sigmundsson et al. (2005); Sigurdsson (1970); Soosalu and Einarsson (1997); Stefánsson (1966); Tibaldi et al. (2013); Villemin et al. (1994). The detailed dataset of the Iceland stress map is provided in the supplementary material. In the following sections we briefly describe each individual stress indicator used for the Iceland stress dataset.

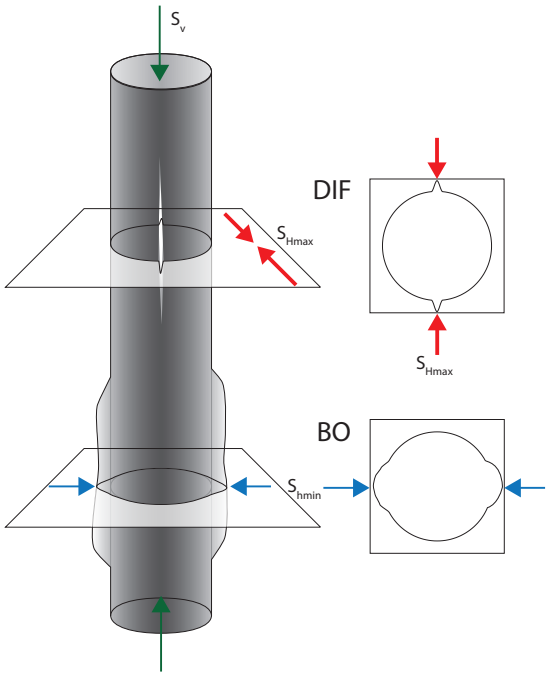

Figure 2: A vertical borehole section with stress indicator pairs. Top: Drilling induced fractures (DIFs) are narrow vertical fractures which indicate the orientation of S_{Hmax}. Bottom: Borehole Breakouts (BOs) are broad vertical widened zones of the borehole which indicate the orientation of S_{hmin}. These two features occur diametrically on both sides of the borehole wall.

2.1. Borehole data

The possibility to determine the in-situ stress orientation from failure of borehole walls was first recognised by Bell and Gough (1979) in Alberta, Canada. They showed that if the stresses around a borehole exceed the strength of the rock, some pieces of the borehole wall spall off and the borehole is elongated in one orientation. According to Kirsch (1898) and Scheidegger (1962) the highest stresses around a circular hole are encountered perpendicular to the orientation of maximum compression (S_{Hmax}). These resulting broad elongated zones of so called borehole breakouts (BO, see Fig. 2) indicate the orientation of minimum horizontal stress (S_{hmin}) which is perpendicular to S_{Hmax} under the assumption that the vertical stress (S_v) is one of the principal stresses (Bell and Gough, 1979).

Furthermore, if the minimum circumferential stress around a borehole wall is smaller than the tensile strength of the rock, drilling induced fractures (DIF, see Fig. 2) occur (Aadnoy, 1990; Aadnoy and Bell, 1998). Therefore drilling induced

fractures are recognised as an indicator for the orientation of S_{Hmax} as well (Wiprut et al., 1997; Bell, 1996; Sperner et al., 2003).

Acoustic image logs provide a picture of the borehole wall based on acoustic contrast of borehole wall and fluids. Borehole breakouts usually appear as broad vertical zones of a low acoustic amplitude on opposite sides of the borehole wall (separated by 180°) while drilling induced fractures are indicated by narrow vertical zones of low amplitude (Fig. 3). A pair of DIFs or BOs on opposite sides of the borehole wall is considered as a single feature. Since the shapes of BOs and DIFs depend on rock strength and the elastic properties of rocks and these features are time dependent, incipient breakouts form at the initial stage of the formation of borehole breakouts (Aadnoy and Bell, 1998).

Iceland's volcano-tectonic setting results in large geothermal resources which are extracted by various boreholes (Ragnarsson, 2015). In 2002 through 2015 the Iceland GeoSurvey (ÍSOR) ran borehole image logs in 57 geothermal and scientific boreholes mainly in the South Iceland Lowlands and around Akureyri and Krafla in the North (see Fig. 4 for locations). From these data we collected and analysed 37 km of acoustic image logs. Most of them are slightly deviated from vertical (< 10°) which still allows the interpretation of stress related features in every stress regime (Mastin, 1988; Tingay et al., 2005; Peška and Zoback, 1995).

27 boreholes contained at least one BO or one DIF (Table 1, Fig. 4). In the case that both BOs and DIFs are found in the same well, the independently inferred S_{Hmax} orientations are generally in good agreement with each other (Table 1). In addition to the newly analysed borehole images 3 BOs and 1 DIF from published articles were included. In the analysed boreholes stress indicators are mainly found between the surface and 1 km depth. Some few BOs/DIFs are located in deeper sections of the boreholes with a maximum depth of 2.34 km in well RN-34 on the Reykjanes peninsula (Fig. 4). Thus borehole stress data bridge the gap between shallow stress indicators from geological data and focal mechanism solutions at greater depth.

Table 1 shows the results of image log interpretation and observed BOs/DIFs in the studied wells. 11 data records have a A-C quality and 25 data records have a D quality. The high number of low quality data records is partly related to the challenges of well-logging in a high temperature and igneous environment resulting in a partly poor image quality. Special tools adapted to high temperatures are required and can only remain in the well for a short time period (Ásmundsson et al., 2014). In addition, in some of the studied wells image tools were not centralised and produced low quality images with numerous vertical artefacts which do not allow a reliable detection of BOs and DIFs.

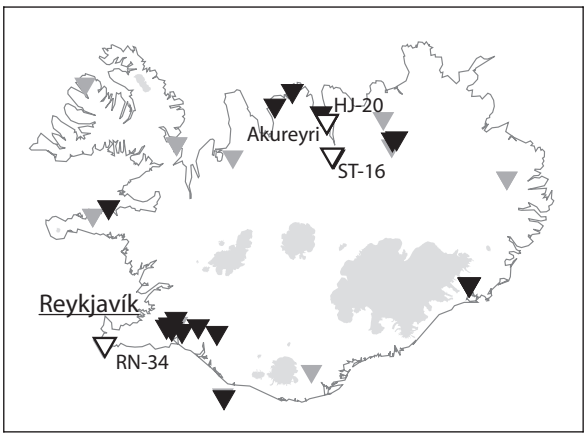

Figure 4: The location of geothermal boreholes with acoustic image logs. The black and grey triangles denote the location of boreholes with and without stress indicators (based on our image log analysis) respectively. The white triangles show the location of borehole HJ-20 Hjalteyri, ST-16 Sigtún (Fig. 3) as well as in RN-34 Reykjanes.

2.2. Focal mechanism solutions

Focal mechanism solutions of earthquakes have been used to infer stress information, both orientation and relative magnitudes, in the deeper part of the earth's crust which is beyond common drilling plans (Sbar and Sykes, 1973; Gephart and Forsyth, 1984; Zoback, 1992; Heidbach et al., 2010). The orientation of S_{Hmax} is estimated from the principal strain axes of the double couple components of the focal mechanism (McKenzie, 1969; Barth et al., 2008). However, these axes are not necessarily reliable proxies for the stress axis orientation (McKenzie, 1969; Célérier, 2010; Heidbach et al., 2010). Therefore, single focal mechanism solutions are never eligible for a quality better than C in the WSM database (Heidbach et al., 2010; Barth et al., 2008). A stress determination though the averaging of several focal mechanism's P, B, and T axes (FMA) is less reliable and is hence assigned D quality.

Between 1994 through 2007 250,000 seismic events were recorded by the Iceland Meteorological

Table 1: Stress indicators from the analysed acoustic borehole images of A-D Quality. All the information required for the WSM quality ranking is included in the Table. Azimuth: Interpreted orientation of S_{Hmax}. Number: The amount of recognised feature pairs (BOs or DIFs) in a single well. S.D.: Standard deviation calculated according to the circular statistics of bi-polar data by Mardia (1972) with a weighting depending of the length (short: L) of the feature. Length: The added length of the fractured borehole sections. Top and Bottom: The depth of the uppermost and lowermost stress indicator found in the borehole. Depth: The mean between top and bottom. Date: Date of the tool run.

Borehole ID	Latitude	Longitude	Azimuth	Type	Depth [km]	Quality	Location	Date	Number	S.D.	Length [m]	Weighting	Top [m]	Bottom [m]
HH-08	63.425023	-20.25904	133	BO	1.05	C	Vestmannaeyjar	20050415	11	13	22	L	789	1719
RN-34	63.83951	-22.660869	36	BO	1.95	C	Reykjanes	20150328	15	12	25	L	1412	2628
RN-34	63.83951	-22.660869	47	DIF	2.45	B	Reykjanes	20150328	20	9	40	L	2317	2612
KH-34	63.98881	-20.44006	67	BO	0.04	D	Kaldárholt	20050322	1	0	2	L	38	40
KH-34	63.98881	-20.44006	109	DIF	0.2	D	Kaldárholt	20050322	2	2	3	L	55	390
SO-01	63.995165	-21.13729	47	DIF	0.32	D	Sogn/Ölfus	20050322	3	13	6	L	314	325
HE-21	64.008906	-21.3438	41	BO	1.67	D	Hellisheiði	20060215	11	14	16	L	1608	1748
HE-21	64.008906	-21.3438	67	DIF	1.35	B	Hellisheiði	20060215	53	14	123	L	912	1812
HE-58	64.033132	-21.376734	35	DIF	1.9	D	Hellisheiði	20150830	3	15	5	L	1609	2200
HN-01	64.026124	-21.45102	45	BO	0.9	C	Hellisheiði	20050405	20	22	26	L	866	977
HN-01	64.026124	-21.45102	44	DIF	0.85	D	Hellisheiði	20050405	7	18	10	L	768	977
HK-15	64.041	-20.81377	8	BO	0.1	C	Grímsnes	20060303	33	15	25	L	37	183
HN-12	64.044597	-21.38636	84	DIF	1.5	D	Hellisheiði	20101021	7	21	11	L	1152	1878
HN-16	64.045106	-21.3862	86	DIF	2.06	D	Hellisheiði	20101018	6	12	9	L	2021	2187
NJ-28	64.098521	-21.270345	107	DIF	1.05	D	Nesjavellir	20150625	5	9	11	L	1029	1057
HF-01	64.391916	-15.34195	151	DIF	0.6	D	Hoffell	20130221	10	11	17	L	424	805
ASK-29	64.393293	-15.343563	130	BO	0.11	D	Hoffell	20120926	6	16	6	L	103	123
ASK-57	64.393898	-15.34267	4	BO	0.28	D	Hoffell	20120926	1	0	1	L	283	284
ASK-122	64.393778	-15.33175	65	DIF	0.35	D	Hoffell	20150924	7	14	13	L	338	375
HO-02	65.04501	-22.77176	60	BO	0.36	D	Stykkishólmur	20070215	1	0	4	L	366	370
ST-16	65.5519	-18.07022	127	BO	0.35	C	Sigtún/Eyjafjörður	20050126	28	9	37	L	111	671
ST-16	65.5519	-18.07022	140	DIF	0.4	D	Sigtún/Eyjafjörður	20050126	5	7	16	L	329	508
BO-3	65.562966	-18.10464	107	DIF	0.07	D	Botn	20130122	3	13	10	L	60	80
KV-01	65.692163	-16.81934	29	BO	1.43	D	Krafla	20060803	1	0	1	L	1435	1437
KV-01	65.692163	-16.81934	164	DIF	1.43	D	Krafla	20060803	2	8	2	L	1432	1435
K-18	65.702026	-16.73063	17	BO	0.74	D	Krafla	20081118	2	4	6	L	733	750
HJ-17	65.855115	-18.2105	151	DIF	0.15	D	Hjalteyri	20020221	2	11	2	L	122	170
HJ-13	65.855337	-18.21303	145	DIF	0.06	D	Hjalteyri	20020220	1	0	3	L	62	65
HJ-20	65.856089	-18.21142	141	BO	1	D	Hjalteyri	20050202	4	8	12	L	784	1176
HJ-20	65.856089	-18.21142	144	DIF	0.75	A	Hjalteyri	20050202	60	11	136	L	352	1346
HJ-15	65.859457	-18.21754	154	DIF	0.2	D	Hjalteyri	20020223	1	0	2	L	204	207
ARS-32	65.931479	-18.33783	163	BO	0.75	D	Árskógsströnd	20060608	6	19	6	L	668	842
ARS-32	65.931479	-18.33783	173	DIF	0.55	C	Árskógsströnd	20060608	17	14	36	L	206	713
SK-28	65.997822	-19.33668	143	BO	0.5	C	Hrolleifsdalur	20051008	55	25	137	L	240	821
SD-01	66.127507	-18.96229	146	BO	0.45	D	Skarðdalur/ Tröllaskagi	20100925	2	3	3	L	430	537
SD-01	66.127507	-18.96229	140	DIF	0.5	B	Skarðdalur/ Tröllaskagi	20100925	20	11	69	L	319	687

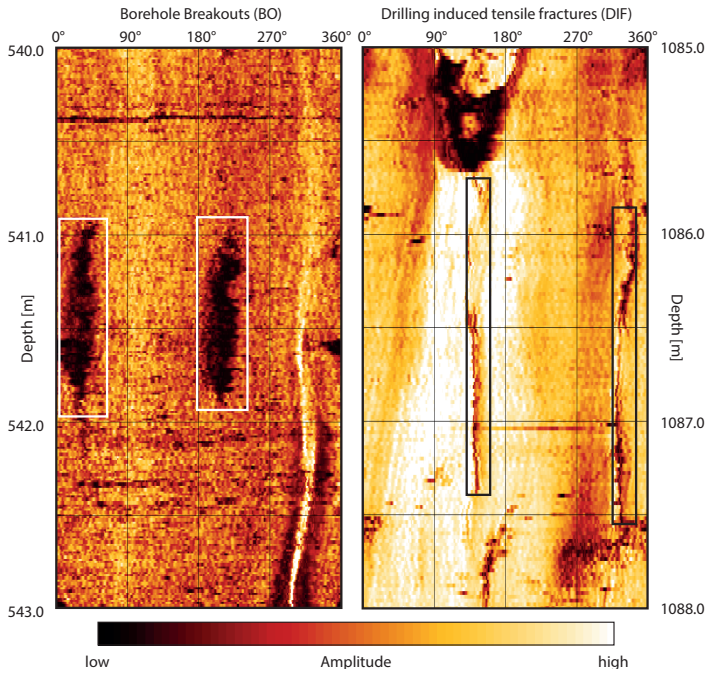

Figure 3: Borehole related stress indicators in acoustic image logs. Left: Borehole breakouts (BOs) in well ST-16 Sigtún close to Akureyri. The inferred overall orientation of S_{Hmax} from BOs is 127° in this well. Right: Drilling induced fractures (DIFs) in well HJ-20 Hjalteyri close to Akureyri. The inferred overall orientation of S_{Hmax} from DIFs is 144° in this well. The location of the two wells is shown in Figure 4.

Office with 11 events of M > 5 (Einarsson, 1991, 2008; Jakobsdóttir et al., 2002; Jakobsdóttir, 2008; Einarsson et al., 1977; Keiding et al., 2009). The detection threshold in this time frame has been between M_l=2 and M_l=0 depending on the region (Jakobsdóttir, 2008). Focal mechanism solutions were publicly available for only a fraction of the recorded seismic events.

Presumably especially in Iceland many seismic events are related to volcanic eruptions or dyke intrusions and thus are potentially spatially and temporally restricted manifestations of the stress field (e.g. Roman et al., 2004; Sánchez et al., 2004; Einarsson, 1991; White et al., 2011). Hence they do not necessarily represent the long-term stress field but only short-term fluctuations of a perturbed regional stress field. In addition, such events may have a low double-couple and high compensated linear vector dipole (CLVD) component (Nettles and Ekström, 1998). That means the main strain component is due to an inflation or deflation above some pressure source in contrast to a double-couple mechanism (Nettles and Ekström, 1998; Ekström, 1994). Therefore events which can be spatially and temporally attributed to a volcanic eruption or rifting event are assigned E quality. However, seismic events which are only located at a volcano but cannot be linked to an eruption remain with a quality C. In the Vatnajökull area several thrust faulting events were recorded during an inter-volcanic period. Nettles and Ekström (1998) and Einarsson (1991) suggest that these events are a movement of the Barðabunga caldera rim. Hence they are not directly temporarily related to a volcanic eruption and assigned the quality C.

Furthermore, the phenomenon of induced seismicity in geothermal reservoirs is reported in Iceland (Flóvenz et al., 2015). The stress field in geothermal or hydrocarbon reservoirs can change significantly due to depletion and/or reinjection (Segall and Fitzgerald, 1998; Martínez-Garzón et al., 2013). Hence, focal mechanisms of seismicity located in the vicinity or within active reservoirs are prone to exhibit a perturbed stress state compared to the virgin in-situ stress state. Therefore seismic events which are in spatial and temporal proximity to e.g. dams or geothermal power plants are identified as potentially induced and are assigned E quality as well.

In addition to single focal mechanism solutions

(FMS) or an average of FMS (FMA), inversions of focal mechanisms (FMF) can be performed (e.g. Gephart and Forsyth, 1984; Angelier, 1984). Generally results from inversions provide high quality (A or B) stress data records (e.g. Keiding et al., 2009; Kristjánsdóttir, 2013). However, the inversions of focal mechanism solutions performed by Bergerat et al. (1998); Garcia et al. (2002); Angelier et al. (2004), and Plateaux et al. (2014) show the existence of two spatially or temporally different local stress fields. Due to the high quality of the inversions they are included in the database anyway but assigned E quality since these two stress fields cannot be distinguished.

2.3. Geological indicators

Geological indicators of past fault slip events can also provide information on the stress state and the data reliability is equal in comparison to other methods (Sperner et al., 2003). However, to prevent a mix of palaeo-stress and contemporary stress data records, geological indicators are generally not allowed to be older than Quaternary, i.e. not older than 2.85 Ma (Zoback, 1992). Sometimes the age of a fault slip or dyke intrusion is measured (e.g. radiocarbon dating), the relative age deduced by the stratigraphy (e.g. in Bergerat and Angelier, 1998), or the maximum age of the rock is otherwise known (e.g. in Bergerat and Plateaux, 2012). If this is not the case geological maps can provide information of the age of the indicators. Note that the rule applies to the age of the fault slip and not the age of the rock, in case where they can be distinguished.

In the new Iceland Stress Map a large amount of data records are provided by geological indicators, i.e. stress tensors inferred from fault slip data. This is due to the extensive work on the stress inversions of fault data (GFI) by J. Angelier, F. Bergerat & A. Guðmundsson undertaken in Iceland (e.g. Bergerat et al., 1990, 1998; Angelier et al., 2004).

We assessed geological indicators (GFI) following strictly the WSM quality ranking scheme (Heidbach et al., 2010; Sperner et al., 2003). Zoback (1992) discusses the possible necessity to alter the age restriction according to the tectonic setting. In case two or more different temporally successive stress states are inferred in the exact same location and both originate in the Quaternary only the youngest can be taken into account in this compilation (as is the case in e.g. Bergerat and Angelier, 1998). In several instances, stress indicators from fault slip data are in close proximity to similarly oriented stress indicators which are definitely from the currently active stress field (e.g. a borehole breakout or focal mechanism solution). Their similar orientation is at least an indicator that the age restriction also applies in Iceland. Even though local stress perturbations do occur due to the presence of local structures (Rajabi et al., 2016; Heidbach et al., 2007) hence different S_{Hmax} orientations in close spatial proximity must not be judged as unreliable.

2.4. Vent alignments

Nakamura (1977) was one of the first to recognise the alignment of volcanic vents, eruptive fissures, and dykes (GVAs) as stress indicators. GVAs are always related to volcanic eruptions which tend to be easier to date compared to fault slip, since often the age of volcanic eruptions are known.

The high volcanic activity in Iceland allows inclusion of young eruptive fissures, vent alignments and dykes from the Quaternary. We therefore included 17 GVAs produced by recent volcanic activities (even in historic times, Thordarson and Larsen 2007). The data originates in geological mapping campaigns and is also displayed in the Geologic Map of Iceland – Bedrock (Hjartarson and Sæmundsson, 2014). Table 2 shows the stress orientations inferred from eruptive fissures mainly deduced from geologic mapping also presented in the map by Hjartarson and Sæmundsson (2014). They are quality ranked according to the WSM criteria shown in Table 3.

2.5. Further stress indicators

In total 25 overcoring (OC) stress measurements are available throughout Iceland. Due to their shallow depth (0 - 30 m) the inferred stress state may be highly influenced by local topography or strength contrasts. Therefore the data records are assigned to E quality. Previous data records from the WSM 2008 which were assigned a different quality according to an outdated version of the ranking scheme were updated.

In addition 9 S_{Hmax} orientations are available from hydraulic-fracturing (HF). Previously listed HF data records were revisited and assigned a quality according to the most recent quality ranking scheme.

3. Stress map & pattern of Iceland

The new compilation of stress data for Iceland has 495 data records with 318 having A-D and 188

Table 2: Newly included volcanic vent and fissure alignments (GVAs) which are also shown in Hjartarson and Sæmundsson (2014). The required information for the World Stress Map as well as the age of the most recent eruption of the associated (central) volcano is listed. Number: The amount of parallel vent/fissure alignments. Vents: The overall number of vents/fissures which are considered. In case of parallel alignments the standard deviation is calculated according to the circular statistics of bi-polar data by Mardia (1972).

Latitude	Longitude	Azimuth	Quality	Location	Number	S.D.	Vents	Type	Last eruption/ rifting event
63.43	-20.2	45	C	Vestmannaeyjar	1		5	vents	1973 A.D.[a]
63.82	-18.83	18	C	Eldgjá (South)	1		6	fissures	934-940 A.D.[a]
63.9	-21.8	56	B	Reykjanes	4	5	21	vents	1231 A.D.[b]
63.94	-18.65	43	C	Eldgjá (Middle)	1		5	fissures	934-940 A.D.[a]
64.1	-18.3	35	C	Eldgjá (North)	1		9	fissures	934-940 A.D.[a]
64.25	-18.6	33	B	Veiðivötn	4	13	67	fissures	1477 A.D.[a]
64.29	-20.84	43	C	Þjófahraun	1		11	fissures	3600 B.P.[c]
64.4	-20.5	47	C	Langjökull	2	3	10	vents	950 A.D.[c]
64.75	-16.6	30	C	Kverkfjöll	1		7	fissures	9000 B.P.[b]
64.8	-17.3	22	B	Dyngjuháls	3	6	28	fissures	1902-1903 A.D.[e]
65	-17.15	29	C	Trölladyngja/ Frambruni	1		8	fissures	1300 A.D.[f]
65.15	-16.6	21	C	Askja	1		14	vents	1961 A.D.[b]
65.4	-16.8	9	C	Fremrinámur	1		9	vents	4000 B.P.[d]
65.5	-16.45	8	C	Nýjahraun	2	6	16	fissures	1874-75 A.D.[d]
65.6	-16.8	8	B	Reykjahlíð	4	2	16	fissures	1975-1984 A.D.[a]
65.7	-16.8	6	C	Krafla	1		10	fissures	1975-1984 A.D.[a]
65.9	-16.35	11	C	Hólssandur	1		7	fissures	Holocene[g]

[a] Thordarson and Larsen 2007, [b] Haflidason et al. 2000, [c] Sinton et al. 2005, [d] Sigurdsson and Sparks 1978, [e] Björnsson and Einarsson 1990, [f] Hjartarson 2003, [g] Hjartarson and Sæmundsson 2014

Table 3: The World Stress Map quality ranking scheme version 2008 for borehole breakouts and drilling induced fractures from image logs and volcanic vent alignments (Heidbach et al., 2010). s.d. = standard deviation.

Stress indicator	**A** S_{Hmax} $\pm 15°$	**B** S_{Hmax} $\pm$ 15 - 20°	**C** S_{Hmax} $\pm$20 - 25°	**D** S_{Hmax} $\pm$25 - 40°	**E** S_{Hmax} $>\pm 40°$
Borehole Breakouts	$\geq$ 10 distinct breakout zones and combined length $\geq$ 100 m in a single well with s.d. $\leq 12°$	$\geq$ 6 distinct breakout zones and combined length $\geq$ 40 m in a single well with s.d. $\leq 20°$	$\geq$ 4 distinct breakouts and combined length $\geq$ 20 m with s.d. $\leq 25°$	$<$ 4 distinct breakouts or $<$ 20 m combined length in a single well with s.d. $\leq 40°$	Wells without reliable breakouts or s.d. $> 40°$
Drilling induced fractures	$\geq$ 10 distinct fracture zones in a single well with a combined length $\geq$ 100 m and s.d. $\leq 12°$	$\geq$ 6 distinct fracture zones in a single well with a combined length $\geq$ 40 m and s.d. $\leq 20°$	$\geq$ 4 distinct fracture zones in a single well with a combined length $\geq$ 20 m and s.d. $\leq 25°$	$<$ 4 distinct fracture zones in a single well or a combined length $<$ 20 m and s.d. $\leq 40°$	Wells without fracture zones or s.d. $> 40°$
Volcanic Vent Alignment	$\geq$ 5 Quaternary vent alignments or "parallel" dikes with s.d. $\leq 12°$	$\geq$ 3 Quaternary vent alignments or "parallel" dikes with s.d. $\leq 20°$	Single well-exposed Quaternary dike or Single alignment with $\geq$ 5 vents	Volcanic alignment inferred from $<$ 5 vents	

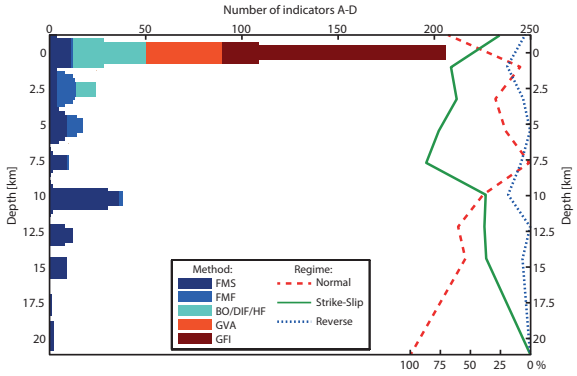

Figure 5: The depth distribution of the 318 stress indicators (A-D quality) is displayed here. The cluster of seismic events around a depth of 10 km is biased since many of the events with an uncertain depth were assigned this depth arbitrarily. The data is colour coded according to the type of the indicator. The width of the bar indicates the quality of the data from A (thick/left) to D (thin/right). Please note that the colour coding is independent of the width of the bar in this plot. In addition the variation of the stress regime with depth is shown on the right side.

Table 4: An overview of the quality and type of all stress indicators in the designated area (N: 62°- 68°, W: 11°- 26°). They include the revisited and re-ranked data from the WSM 2008 as well as the newly analysed data from acoustic image logs, the alignments of volcanic craters and fissures, and data records from literature research.

		Quality					
		A	B	C	D	E	Total
Type	FMF	15	7	-	-	14	36
	FMS	-	-	63	22	90	175
	FMA	-	-	-	9	-	9
	BO	-	-	6	13	30	49
	DIF	1	3	1	15	1	21
	HF	-	1	2	6	-	9
	OC	-	-	-	-	25	25
	GFI	1	11	40	63	14	129
	GVA	1	11	25	2	3	42
	Total	18	33	137	130	177	495

A-C quality (Table 4, Figs. 1 & 5). Most of the A-D quality data records are from focal mechanism solutions (35%) and geological fault inversions (26%). Borehole related indicators (BOs, DIFs, HFs) have a share of 20% while the alignments of volcanic vents, fissures and craters contribute with 8%. The inversion of several focal mechanism solutions make up 7% of the dataset.

56% of the data records are from the depth range of 0 to 1.25 km (Fig. 5). These are mainly geological stress indicators which are either exhumed faults or surface manifestations of the stress field. Most borehole indicators are in the same depth range. Even some very shallow focal mechanism solutions and inversions of several focal mechanisms are located in that depth range. Around 2.5 km depth stress indicators from deep boreholes and earthquake related indicators are equally abundant. Below that depth, focal mechanism solutions of seismic events are the only available stress indicators. The peak of events around 10 km is artificial because many focal mechanisms of small magnitude seismic events are assigned this depth as a default value if the depth cannot be estimated otherwise.

Some stress indicators (e.g. focal mechanism solutions, fault inversions) allow characterisation of the Andersonian faulting type of the stress field (Anderson, 1905, 1951). The method to derive the type of faulting is described by Zoback (1992). Figure 5 shows that normal faulting prevails at the surface. However, within the first kilometre this changes. In the following topmost 10 km a strike slip regime is dominant. With a further increase in depth the normal faulting regime prevails. Indicators for a reverse faulting regime are observed in all depths in a relatively small abundance. Nevertheless, around 1 km and 10 km depth they have a significant share.

The prevailing orientation of S_{Hmax} in Iceland inferred from A-C quality ranked data records is determined according to circular statistics of bipolar data (Mardia, 1972) which shows a mean S_{Hmax} orientation of 18°± 35° for the entire dataset. A closer look at Figure 1 demonstrates four predominant regional orientations of S_{Hmax}. In the Southwest and the Southern Iceland Lowlands S_{Hmax} is oriented approximately NE-SW (Fig. 6). In the Northern Volcanic Zone (north of the Vatnajökull glacier) which is presently the active rift zone, S_{Hmax} has almost N-S orientation (Fig. 7). S_{Hmax} is rotated by about 20° to NNE-SSW in the easternmost part of Iceland (Fig. 7). In Northern Iceland S_{Hmax} is rotated from the N-S orientation in the Northern Volcanic Zone to a predominant NNW-SSE orientation (Fig. 8). Finally in the Westfjords the S_{Hmax} trend is approximately NW-SE oriented (Fig. 9). For these four subsets the standard deviation for A-D quality data is between 19° and 29° which is comparable to other regional stress investigations (e.g. Pierdominici and Heidbach, 2012;

Reiter et al., 2014; Reinecker et al., 2010).

Generally the standard deviation of the mean S_{Hmax} orientation of stress data records with A-C quality is found to be within ±25° (see rose diagrams in Figures 1, 6, 7, 8, & 9). If D quality data records are included the mean S_{Hmax} orientation changes by ≤4°. The standard deviation increases by approximately 5° reflecting that D quality data introduces more noise to the dataset. Therefore D quality data should not be used individually for a local stress field analysis. Surprisingly the standard deviation decreases by 1° with the introduction of 11 D quality data records in North Iceland. 10 of these data records are from boreholes and their quality depends on the short length of the feature and/or missing information on the standard deviation. These circumstances show that a well-picked distinct single feature in a borehole provides valuable information on the orientation of S_{Hmax}.

The types of available stress indicators varies in the different subsets. While all types of indicators are represented close to the plate boundary, in the Westfjords and Eastfjords the stress state is mainly derived from geological indicators and boreholes. That means that in those regions the information on the stress field is based mainly on shallow data.

Apart from lateral variations of the orientation of S_{Hmax}, the possibility of a vertical layering exists (Cornet and Röckel, 2012; Gudmundsson, 2002; Heidbach et al., 2007). In some regions, mainly sedimentary basins, moderate (Reiter et al., 2014; Reiter and Heidbach, 2014) or significant (Röckel and Lempp, 2003; Roth and Fleckenstein, 2001; Rajabi et al., 2016) stress rotations occur with depth. For example, Rajabi et al. (2016) reported significant rotation of the S_{Hmax} orientation with depth in the Clarence-Moreton Basin of eastern Australia due to presence of geological structures including intrusions of igneous rocks into sedimentary successions.

It is indicated by the propagation of dykes, that such a layering also exists in Iceland on a local scale (Gudmundsson, 2002, 2003). To find regional-scale depth-dependent differences in the S_{Hmax} orientation we compiled surface data (GFI, GVA) as well as intermediate (0.2-2 km) borehole indicators (BO, DIF) and deep (2-20 km) focal mechanism solutions (Fig. 5). In all areas where more than one type of indicator is available, the orientation of S_{Hmax} remains consistent with depth which highlights the independence from the type of stress indicator and the vertical homogeneity of S_{Hmax} throughout the crust. Thus a potential regional-scale depth-dependency of S_{Hmax} is not observed.

4. Discussion

This study presents the first comprehensive and systematic compilation of the present-day tectonic stress in Iceland where all results are ranked based on a quality ranking scheme for the in-situ stress state. A high density of data records is achieved on the Reykjanes peninsula, in South Iceland, East Iceland, and the Akureyri area and Tjörnes Fracture Zone in North Iceland (Fig. 1). Few or no data records are available around Hofsjökull, Langjökull in the western Highlands, on the Snæfellsnes peninsula, and in the Westfjords (Fig. 1). Based on the available data from this compilation the orientation of the maximum compressive stress (S_{Hmax}) in Iceland is organised in four subsets and is consistent with the main plate boundaries in the region. This highlights the role of different plate boundary forces in the stress pattern of Iceland (Fig. 10). Furthermore the highly dynamic geological setting of Iceland is reflected in the stress field by effects of eruptions, geothermal activity, and rifting events.

4.1. Regional stress pattern

In the South-West a ridge parallel S_{Hmax} orientation can be observed along the Reykjanes Ridge (Fig. 1) which has the Eurasian plate to the East and the North American plate to the West (Einarsson, 2008; Bird, 2003). At the Reykjanes peninsula where the ridge makes landfall S_{Hmax} remains mostly ridge parallel (Figs. 1 & 6). This pattern of S_{Hmax} is consistent with observations by e.g. Sykes (1967) and Wiens and Stein (1984) who show ridge parallel S_{Hmax} close to the spreading centre along divergent plate boundaries in general and especially in the Indian Ocean.

Ridge parallel stress is also indicated further to the North along the WVZ (Fig. 1). The western boundary of the Hreppar microplate is at the WVZ and its northern boundary is the quietest Central Iceland Volcanic Zone (CIVZ) which is not represented by stress indicators here (Einarsson, 2008).

In the South the Hreppar microplate meets the Eurasian plate at the transform SISZ (Einarsson, 2008). This is one of the two areas with the largest seismic events (M=7.2) in Iceland (e.g. Stefánsson et al., 2000; Bergerat and Angelier, 2001). In the SISZ the S_{Hmax} is NNE to NE (Fig. 6) which is

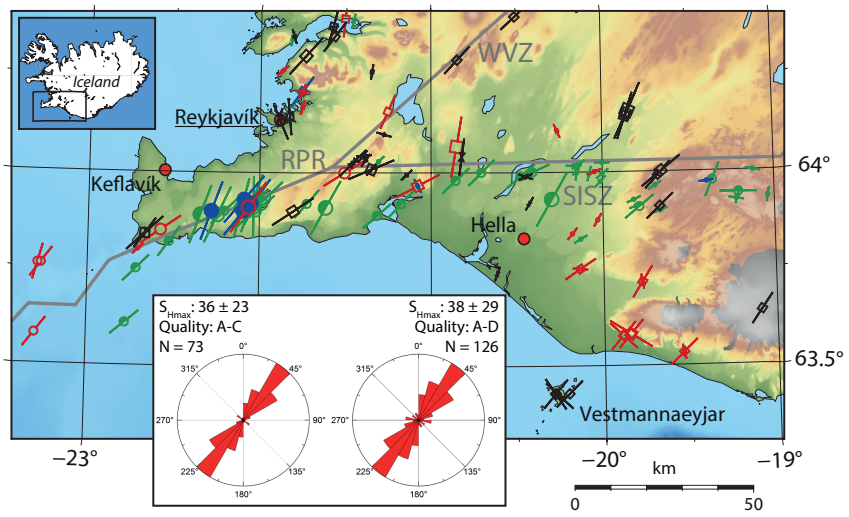

Figure 6: The orientation of S_{Hmax} (A-D Quality) on the Reykjanes peninsula ridge (RPR), the transform South Iceland Seismic Zone (SISZ), and parts of the Western Volcanic Zone (WVZ). Legend is the same as in Figure 1.

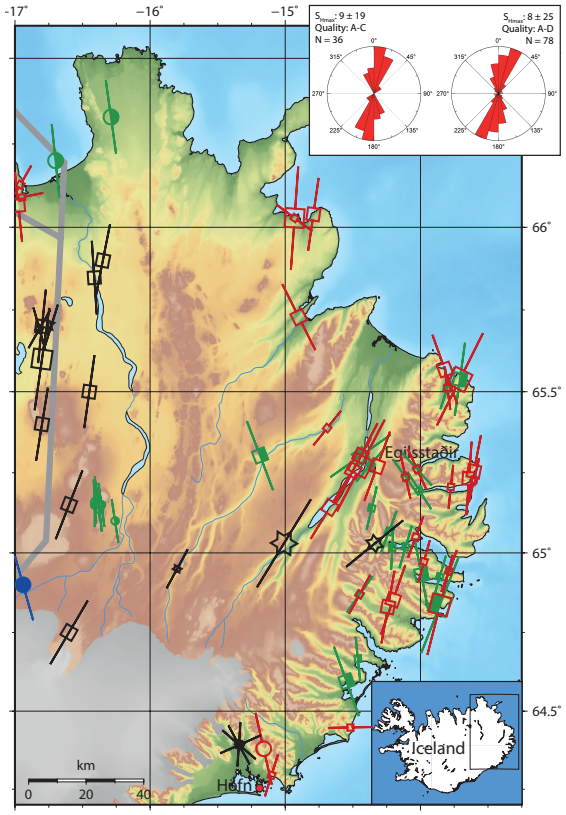

Figure 7: The orientation of S_{Hmax} (A-D Quality) in the Eastern Highlands/Northern Volcanic Zone and the East Fjords. Legend is the same as in Figure 1. Note that mainly surface geological indicators are available in this area.

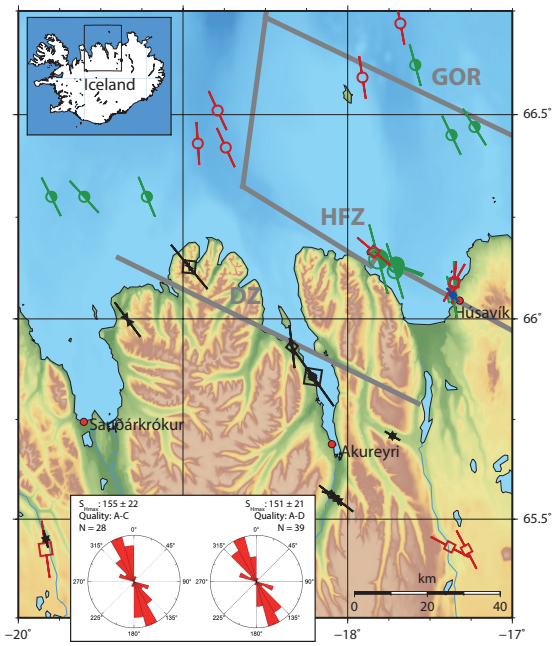

Figure 8: The orientation of S_{Hmax} (A-D Quality) in Northern Iceland. Displayed is the Tjörnes Fracture Zone with the Grimsey oblique rift (GOR), the Húsavík-Flatey-Zone (HFZ), and the Dalvík Zone (DZ). Legend is the same as in Figure 1.

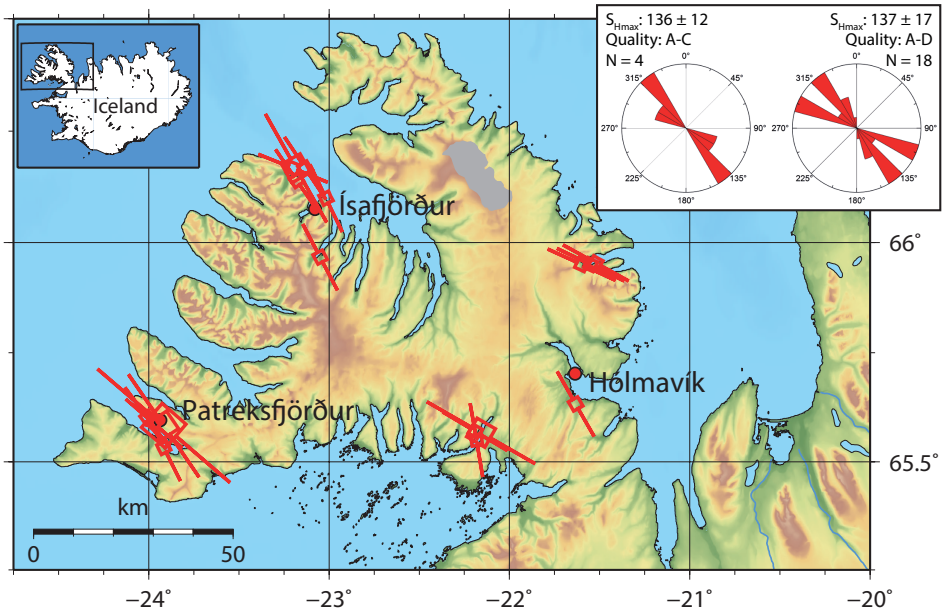

Figure 9: The orientation of S_{Hmax} (A-D Quality) in the Westfjords. In the oldest area of Iceland (10-16 Ma, Moorbath et al. 1968; McDougall et al. 1984) S_{Hmax} is rotated from rift parallel to rift normal. Legend is the same as in Figure 1. Note that only surface geological indicators are available in this area.

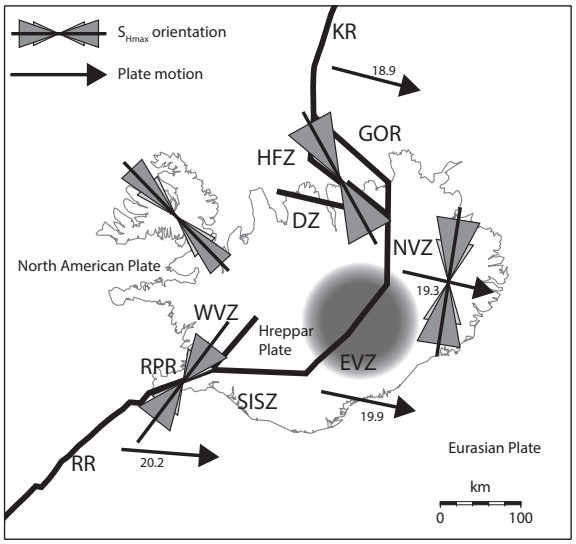

Figure 10: A simplified tectonic map of Iceland with the mean orientations of S_{Hmax} in the four stress provinces estimated from A-D quality data records (black lines). The standard deviation from A-C quality is shown by the large dark grey areas while the light grey areas show the standard deviation from A-D quality. The plate boundaries are from Einarsson (2008) & Bird (2003). The plate motion (mm/yr) is indicated by black arrows relative to the fixed North American plate (Geirsson et al., 2006). The continental plates and the approximate location of the hotspot (grey circle, Wolfe et al., 1997) are indicated. Furthermore the tectonic features are labelled as follows according to Einarsson (2008): RR: Reykjanes Ridge, RPR: Reykjanes peninsula ridge, WVZ: Western Volcanic Zone, SISZ: South Iceland Seismic Zone, EVZ: Eastern Volcanic Zone, NVZ: Northern Volcanic Zone, DZ: Dalvík Zone, HFZ: Húsavík-Flatey-Zone, GOR: Grimsey-Oblique-Ridge, and KR: Kolbeinsey Ridge.

consistent with the surface ruptures of large earthquakes (e.g. Árnadóttir et al., 2003; Einarsson, 2008).

In the North-East of the SISZ the EVZ and the NVZ are the currently active rift zones (Einarsson, 2008). Most of the rifting events (Laki, Eldgjá, Krafla fires, Holuhraun) and volcanic eruptions (Grimsvötn, Gjálp, Askja, Hekla, Barðabunga) are in these two zones (Sigmundsson et al., 2015; Thordarson and Larsen, 2007). This activity is related to the current location of the centre of the hotspot which is considered to be beneath the Vatnajökull glacier at the transition from the EVZ to the NVZ (e.g. Wolfe et al., 1997; Ito et al., 2003, Fig. 10). The S_{Hmax} is found to follow the orientation of the EVZ and NVZ which are considered as the plate boundary from NE-SW in the South to N-S in the North (Fig. 1). This pattern is also observed at some distance along the Icelandic east coast (Fig. 7).

In the North, the TFZ connects the NVZ with the Kolbeinsey Ridge north of Iceland (Sæmundsson, 1974, 1979; Einarsson, 1991; Garcia, 2003; Stefánsson et al., 2008). The spreading is distributed between the Dalvík Zone (DZ), the Húsavík-Flatey-Zone (HFZ) and the Grimsey Oblique Rift (GOR) (Sæmundsson, 1974). This is the second area with large magnitude seismic events in Iceland (Jakobsdóttir, 2008) and shows a NNW - SSE trend for the S_{Hmax} orientation which is mainly inferred from focal mechanism solutions (Fig.8).

In the Westfjords which are the oldest part of Iceland (10-16 Ma, Moorbath et al. 1968; McDougall et al. 1984) and also partly on the Snæfellsnes peninsula a rotation of S_{Hmax} from ridge parallel towards ridge perpendicular is observed (Figs. 9 & 1). This rotation is interpreted as the transition from the ridge parallel stress orientation to the common intraplate stress orientation (Wiens and Stein, 1984; Sykes, 1967; Sykes and Sbar, 1974; Müller et al., 1992; Grünthal and Stromeyer, 1992; Gudmundsson et al., 1996). This rotation is expected in some distance from the spreading centre which depends mainly on the composition of the rock and only partly on the age and distance from the ridge (Wiens and Stein, 1984). Such a rotation is also expected to occur off the Icelandic east coast to meet the overall trend of S_{Hmax} observed in Europe (e.g. Grünthal and Stromeyer, 1992; Müller et al., 1992; Heidbach et al., 2007).

Many of the stress indicators recognised in the applied quality ranking, e.g. focal mechanism solutions or borehole breakouts, are manifestations of a stress field which generally can be assumed as the currently active in-situ stress field. Still, seismic events and volcanic eruptions may change the local stress field in a very short time interval (e.g. Reasenberg and Simpson 1992; King et al. 1994; Dieterich et al. 2000). Albeit, these changes induced by seismic events are generally smaller than the regional stress magnitude (Hardebeck, 2010). Hence they are assumed to be within the uncertainty of $S_{Hmax} \pm 15°$ of even the highest quality stress indicators. As well the isostatic rebound from deglaciation is not expected to have an immediate impact on stress orientation (Plateaux et al., 2014).

4.2. Comparison with other observations

A comparison of the orientation of S_{Hmax} with the direction of plate motion (Geirsson et al., 2006) shows that they are in quite large areas perpendicular to each other (Fig. 10). In a more local study Keiding et al. (2009) compared the stress and strain in the Reykjanes peninsula. The stress is determined from the inversion of focal mechanism from earthquake swarms while the strain is derived from GPS data. Keiding et al. (2009) conclude that the minimum horizontal stress (S_{hmin}) is parallel to the maximum horizontal strain $\dot{\epsilon}_{Hmax}$. This also holds for detailed GPS data provided by Árnadóttir et al. (2009). In the Westfjords the orientation of S_{Hmax} is sub-parallel to the plate motion (Fig. 9 and Árnadóttir et al., 2009, Figs 3 & 4).

Extensive maps of surface fissure swarms are available for Iceland (e.g. Gudmundsson 1987; Clifton and Kattenhorn 2006; Hjartardóttir et al. 2009; Einarsson 2010; Hjartardottir et al. 2015). Even though eruptive fissures can be used as stress indicators, surface fissure swarms do not provide information on the stress field but on the deformation (Hjartardottir et al., 2015). The fissure swarms are very similarly oriented to the orientation of the S_{Hmax}. Especially in the NVZ the orientation of the fissure swarms are well in agreement with eruptive fissures and other stress indicators (e.g. Hjartardottir et al., 2015).

5. Conclusion

In this paper we present the first comprehensive and quality ranked compilation of the contemporary stress data in Iceland including the analysis of image logs from 57 geothermal boreholes. In total we compiled 495 S_{Hmax} orientations from different stress indicators. The main contributions to the newly compiled database are from 171 surface geological information, 61 geothermal wells (intermediate-depth), and 175 indicators from focal mechanism solutions of earthquakes (deep). The two key findings of this compilation are: (1) no significant depth-dependent variation in the S_{Hmax} orientation ($\pm 25°$) is observed while the stress regime changes with depth. (2) four distinct contemporary stress provinces are present in Iceland. The stress provinces are in agreement with the large-scale regional tectonic setting.

Acknowledgement

The authors would like to thank Romain Plateaux and two anonymous reviewers for their comments which significantly improved the manuscript. Furthermore the authors would like to thank Orkuveita Reykjavíkur, RARIK, Norðurorka, Landsvirkjun, HS Orka, and Skagafjarðarveitur for the permission to publish the televiewer data. The research leading to these results has received funding from the European Community's Seventh Framework Programme under grant agreement No. 608553 (Project IMAGE). With respect to this we like to thank David Bruhn and Ólafur G. Flóvenz. The maps are generated with CASMI (Heidbach and Höhne, 2008) and GMT (Wessel et al., 2013) with topographic data from ETOPO1 (Amante and Eakins, 2009) and bathymetric data from the GEBCO_2014 Grid, www.gebco.net. We also would like to thank Kristján Sæmundsson and Maryam Khodayar who read the manuscript as well as John Reinecker and Sebastian Specht for their support in technical issues. Mojtaba Rajabi's contribution forms TRaX record #344.

References

Aadnoy, B. and Bell, J. (1998). Classification of drilling-induced fractures and their relationship to in-situ stress directions. *The Log Analyst*, (November-December):27–42.

Aadnoy, B. S. (1990). Inversion technique to determine the in-situ stress field from fracturing data. *Journal of Petroleum Science and Engineering*, 4(2):127–141.

Allen, R. M., Nolet, G., Morgan, W. J., Vogfjörd, K., Nettles, M., Ekström, G., Bergsson, B. H., Erlendsson, P., Foulger, G., Jakobsdóttir, S., Julian, B. R., Pritchard,

M., Ragnarsson, S., and Ragnar, S. (2002). Plume-driven plumbing and crustal formation in Iceland. *Journal of Geophysical Research: Solid Earth (1978–2012)*, 107(B8):ESE–4.

Amante, C. and Eakins, B. (2009). ETOPO1 1 Arc-Minute Global Relief Model: Procedures, Data Sources and Analysis. *NOAA Technical Memorandum NESDIS NGDC-24. National Geophysical Data Center, NOAA*.

Anderson, E. (1905). The dynamics of faulting. *Transactions of the Edinburgh Geological Society*, 8:387–402.

Anderson, E. (1951). *The dynamics of faulting*. Oliver and Boyd, Edinburgh, 2 edition.

Andrew, R. E. and Gudmundsson, A. (2008). Volcanoes as elastic inclusions: Their effects on the propagation of dykes, volcanic fissures, and volcanic zones in Iceland. *Journal of Volcanology and Geothermal Research*, 177(4):1045–1054.

Angelier, J. (1984). Tectonic analysis of fault slip data sets. *Journal of Geophysical Research*, 89(B7):5835.

Angelier, J., Bergerat, F., Stefánsson, R., and Bellou, M. (2008). Seismotectonics of a newly formed transform zone near a hotspot: Earthquake mechanisms and regional stress in the South Iceland Seismic Zone. *Tectonophysics*, 447(1-4):95–116.

Angelier, J., Slunga, R., Bergerat, F., Stefánsson, R., and Homberg, C. (2004). Perturbation of stress and oceanic rift extension across transform faults shown by earthquake focal mechanisms in Iceland. *Earth and Planetary Science Letters*, 219(3-4):271–284.

Árnadóttir, T., Jónsson, S., Pedersen, R., and Gudmundsson, G. B. (2003). Coulomb stress changes in the South Iceland Seismic Zone due to two large earthquakes in June 2000. *Geophysical Research Letters*, 30(5):1205.

Árnadóttir, T., Lund, B., Jiang, W., Geirsson, H., Björnsson, H., Einarsson, P., and Sigurdsson, T. (2009). Glacial rebound and plate spreading: results from the first countrywide GPS observations in Iceland. *Geophysical Journal International*, 177(2):691–716.

Ásmundsson, R., Pezard, P., Sanjuan, B., Henninges, J., Deltombe, J.-L., Halladay, N., Lebert, F., Gadalia, A., Millot, R., Gibert, B., Violay, M., Reinsch, T., Naisse, J.-M., Massiot, C., Azaïs, P., Mainprice, D., Karytsas, C., and Johnston, C. (2014). High temperature instruments and methods developed for supercritical geothermal reservoir characterisation and exploitation - The HiTI project. *Geothermics*, 49:90–98.

Barth, A., Reinecker, J., and Heidbach, O. (2008). Stress derivation from earthquake focal mechanisms. Technical report, World Stress Map Project.

Batir, J. (2011). Stress field characterization of the Hellisheiði geothermal field and possibilities to improve injection capabilities. Master thesis, RES - The School for Renewable Energy Science.

Bell, J. (1996). In situ stresses in sedimentary rocks (Part 1): Measurement Techniques. *Geoscience Canada*, 23(2).

Bell, J. and Gough, D. (1979). Northeast-southwest compressive stress in Alberta - evidence from oil wells. *Earth and Planetary Science Letters*, 45(2):475–482.

Bergerat, F. and Angelier, J. (1998). Fault systems and paleostresses in the Vestfirdir Peninsula. Relationships with the Tertiary paleo-rifts of Skagi and Snaefells (Northwest Iceland). *Geodinamica Acta*, 11(2-3):105–118.

Bergerat, F. and Angelier, J. (2001). Mechanisms of the faults of 17 and 21 June 2000 earthquakes in the South Iceland Seismic Zone from the surface traces of the árnes and Hestfjall faults. *Comptes Rendus de l'Académie des Sciences - Series IIA - Earth and Planetary Science*, 333(1):35–44.

Bergerat, F., Angelier, J., and Villemin, T. (1990). Fault systems and stress patterns on emerged oceanic ridges: a case study in Iceland. *Tectonophysics*, 179(3-4):183–197.

Bergerat, F., Gudmundsson, A., Angelier, J., and Rögnvaldsson, S. (1998). Seismotectonics of the central part of the South Iceland Seismic Zone. *Tectonophysics*, 298(4):319–335.

Bergerat, F. and Plateaux, R. (2012). Architecture and development of (Pliocene to Holocene) faults and fissures in the East Volcanic Zone of Iceland. *Comptes Rendus Geoscience*, 344(3-4):191–204.

Bird, P. (2003). An updated digital model of plate boundaries. *Geochemistry, Geophysics, Geosystems*, 4(3):1–52.

Bjarnason, I. T. and Einarsson, P. (1991). Source mechanism of the 1987 Vatnafjöll earthquake in South Iceland. *Journal of Geophysical Research*, 96(B3):4313–4324.

Björnsson, H. and Einarsson, P. (1990). Volcanoes beneath Vatnajökull, Iceland: Evidence from radio echo-sounding, earthquakes and jökulhlaups. *Jökull*, (40):22.

Célérier, B. (2010). Remarks on the relationship between the tectonic regime, the rake of the slip vectors, the dip of the nodal planes, and the plunges of the P, B, and T axes of earthquake focal mechanisms. *Tectonophysics*, 482(1-4):42–49.

Centre, G. D. (1993). GEOFON Seismic Network. Other/Seismic Network.

Clifton, A. E. and Kattenhorn, S. A. (2006). Structural architecture of a highly oblique divergent plate boundary segment. *Tectonophysics*, 419(1):27–40.

Cornet, F. H. and Röckel, T. (2012). Vertical stress profiles and the significance of "stress decoupling". *Tectonophysics*, 581:193–205.

Dieterich, J., Cayol, V., and Okubo, P. (2000). The use of earthquake rate changes as a stress meter at Kilauea volcano. *Nature*, 408(6811):457–460.

Dziewonski, A. M. M., Chou, T.-A., and Woodhouse, J. H. (1981). Determination of earthquake source parameters from waveform data for studies of global and regional seismicity. *Journal of Geophysical Research*, 86(B4):2825.

Einarsson, P. (1979). Seismicity and earthquake focal mechanisms along the Mid-Atlantic plate boundary between Iceland and the Azores. *Tectonophysics*, 55(1-2):127–153.

Einarsson, P. (1987). Compilation of earthquake fault plane solutions in the North Atlantic and Arctic Oceans. In *Recent plate movements and deformation*, pages 47–62.

Einarsson, P. (1991). Earthquakes and present-day tectonism in Iceland. *Tectonophysics*, 189(1-4):261–279.

Einarsson, P. (2008). Plate boundaries, rifts and transforms in Iceland. *Jökull*, (58):35–58.

Einarsson, P. (2010). Mapping of Holocene surface ruptures in the South Iceland Seismic Zone. *Jökull*, 60:121–138.

Einarsson, P., Klein, F., and Björnsson, S. (1977). The Borgarfjördur earthquakes of 1974 in West Iceland. *Bulletin of the Seismological Society of America*, 67(1):187–208.

Ekström, G. (1994). Anomalous earthquakes on volcano ring-fault structures. *Earth and Planetary Science Letters*, 128(3-4):707–712.

Ekström, G., Nettles, M., and Dziewonski, A. (2012). The Global CMT Project 2004 - 2010: Centroid-moment tensors for 13,017 earthquakes. *Physics of the Earth and Planetary Interiors*, 200-201:1–9.

Flóvenz, Ó. G., Ágústsson, K., Guðnason, E. Á., and

Kristjánsdóttir, S. (2015). Reinjection and Induced Seismicity in Geothermal Fields in Iceland. In *Proceedings World Geothermal Congress 2015*, number April, pages 1–15, Melbourne, Australia.

Forslund, T. and Gudmundsson, A. (1991). Crustal spreading due to dikes and faults in southwest Iceland. *Journal of Structural Geology*, 13(4):443–457.

Garcia, S. (2003). *Implications d'un saut de rift et du fonctionnement d'une zone transformante sur les deformations du nord de l'Islande*. Phd-thesis, Université Pierre et Marie Curie.

Garcia, S., Angelier, J., Bergerat, F., and Homberg, C. (2002). Tectonic analysis of an oceanic transform fault zone based on fault-slip data and earthquake focal mechanisms: the Húsavík-Flatey Fault zone, Iceland. *Tectonophysics*, 344(3-4):157–174.

Garcia, S. and Dhont, D. (2005). Structural analysis of the Húsavík-Flatey transform fault and its relationships with the rift system in Northern Iceland. *Geodinamica Acta*, 18(1):31–41.

Geirsson, H., Árnadóttir, T., Völksen, C., Jiang, W., Sturkell, E., Villemin, T., Einarsson, P., Sigmundsson, F., and Stefánsson, R. (2006). Current plate movements across the Mid-Atlantic Ridge determined from 5 years of continuous GPS measurements in Iceland. *Journal of Geophysical Research*, 111(B9):B09407.

Gephart, J. W. and Forsyth, D. W. (1984). An improved method for determining the regional stress tensor using earthquake focal mechanism data: Application to the San Fernando Earthquake Sequence. *Journal of Geophysical Research*, 89(B11):9305.

Green, R. G., White, R. S., and Greenfield, T. (2014). Motion in the north Iceland volcanic rift zone accommodated by bookshelf faulting. *Nature Geoscience*, 7(1):29–33.

Grünthal, G. and Stromeyer, D. (1992). The recent crustal stress field in central Europe: trajectories and finite element modeling. *Journal of Geophysical Research*, 97(B8):11805–11820.

Gudmundsson, A. (1987). Tectonics of the Thingvellir fissure swarm, SW Iceland. *Journal of Structural Geology*, 9(1):61–69.

Gudmundsson, A. (1995). Infrastructure and mechanics of volcanic systems in Iceland. *Journal of Volcanology and Geothermal Research*, 64(94).

Gudmundsson, A. (2002). Emplacement and arrest of sheets and dykes in central volcanoes. *Journal of Volcanology and Geothermal Research*, 116(3):279–298.

Gudmundsson, A. (2003). Surface stresses associated with arrested dykes in rift zones. *Bulletin of Volcanology*, 65(8):606–619.

Gudmundsson, A. (2006). How local stresses control magma-chamber ruptures, dyke injections, and eruptions in composite volcanoes. *Earth-Science Reviews*, 79(1-2):1–31.

Gudmundsson, A., Bergerat, F., and Angelier, J. (1996). Off-rift and rift-zone palaeostresses in Northwest Iceland. *Tectonophysics*, 255(3-4):211–228.

Gudmundsson, A., Bergerat, F., Angelier, J., and Villemin, T. (1992). Extensional tectonics of southwest Iceland. *Bulletin de la Societe Geologique de France*, 163(5):561–570.

Haflidason, H., Eiriksson, J., and Kreveld, S. V. (2000). The tephrochronology of Iceland and the North Atlantic region during the Middle and Late Quaternary: a review. *Journal of Quaternary Science*, 15(1):3–22.

Hagos, L., Shomali, H., Lund, B., Böðvarsson, R., and Roberts, R. (2008). An Application of Relative Moment Tensor Inversion to Aftershocks of the June 1998 Hengill Earthquake in Southwest Iceland. *Bulletin of the Seismological Society of America*, 98(2):636–650.

Haimson, B. and Rummel, F. (1982). Hydrofracturing stress measurements in the Iceland research drilling project drill hole at Reyðarfjörður, Iceland. *Journal of Geophysical Research*, 87(B8):6631–6649.

Haimson, B. and Voight, B. (1977). Crustal stress in Iceland. *Pageoph*, 115:153–190.

Hardebeck, J. (2010). Aftershocks are well aligned with the background stress field, contradicting the hypothesis of highly heterogeneous crustal stress. *Journal of Geophysical Research*, 115(B12):B12308.

Hast, N. (1969). The state of stress in the upper part of the earth's crust. *Tectonophysics*, 8(3):169–211.

Heidbach, O. and Höhne, J. (2008). CASMI – A visualization tool for the World Stress Map database. *Computers & Geosciences*, 34(7):783–791.

Heidbach, O., Reinecker, J., Tingay, M., Müller, B., Sperner, B., Fuchs, K., and Wenzel, F. (2007). Plate boundary forces are not enough: Second- and third-order stress patterns highlighted in the World Stress Map database. *Tectonics*, 26(6):1–19.

Heidbach, O., Tingay, M., Barth, A., Reinecker, J., Kurfeß, D., and Müller, B. (2008). The 2008 release of the World Stress Map.

Heidbach, O., Tingay, M., Barth, A., Reinecker, J., Kurfeß, D., and Müller, B. (2010). Global crustal stress pattern based on the World Stress Map database release 2008. *Tectonophysics*, 482(1-4):3–15.

Hjartardottir, A. R., Einarsson, P., Magnusdottir, S., Bjornsdottir, T., and Brandsdottir, B. (2015). Fracture systems of the Northern Volcanic Rift Zone, Iceland: an onshore part of the Mid-Atlantic plate boundary. *Geological Society, London, Special Publications*.

Hjartardóttir, Á. R., Einarsson, P., and Sigurdsson, H. (2009). The fissure swarm of the Askja volcanic system along the divergent plate boundary of N Iceland. *Bulletin of Volcanology*, 71(9):961–975.

Hjartarson, Á. (2003). Postglacial lava production in Iceland. In *The Skagafjörður Unconformity, North Iceland, and its Geological History. PhD thesis*, pages 95–108. Geological Museum, University of Copenhagen, Copenhagen.

Hjartarson, Á. and Sæmundsson, K. (2014). Geologic Map of Iceland. Bedrock. 1 : 600 000. Technical report, Iceland GeoSurvey.

Ito, G., Lin, J., and Graham, D. (2003). Observational and theoretical studies of the dynamics of mantle plume-mid-ocean ridge interaction. *Reviews of Geophysics*, 41(4):1017.

Jakobsdóttir, S. (2008). Seismicity in Iceland: 1994 - 2007. *Jökull*, (58):1994–2007.

Jakobsdóttir, S., Gudmundsson, G., and Stefánsson, R. (2002). Seismicity in Iceland 1991 - 2000 monitored by the SIL seismic system. *Jökull*, (51):87–94.

Jakobsson, S. (1979). Petrology of recent basalts of the Eastern Volcanic Zone, Iceland. *Acta Natiuralia Islandica*, 26.

Jefferis, R. and Voight, B. (1981). Fracture analysis near the mid-ocean plate boundary, Reykjavík-Hvalfjörður area, Iceland. *Tectonophysics*, 76:171–236.

Jóhannesson, H. and Sæmundsson, K. (1998). Geological Map of Iceland, 1:500,000. Bedrock Geology. Technical report, Icelandic Institute of Natural History and Icelandic Geodetic Survey, Reykjavík.

Keiding, M., Lund, B., and Árnadóttir, T. (2009). Earthquakes, stress, and strain along an obliquely divergent plate boundary: Reykjanes Peninsula, southwest Iceland. *Journal of Geophysical Research*, 114(B9):B09306.

Khodayar, M. and Franzson, H. (2007). Fracture pattern of Thjórsárdalur central volcano with respect to rift-jump and a migrating transform zone in South Iceland. *Journal of Structural Geology*, 29(5):898–912.

King, G., Stein, R., and Lin, J. (1994). Static stress changes and the triggering of earthquakes. *Bulletin of the Seismological Society of America*, 84(3):935–953.

Kirsch, E. G. (1898). Die Theorie der Elastizität und die Bedürfnisse der Festigkeitslehre. *Zeitschrift des Vereines Deutscher Ingenieure*, 42:797–807.

Kristjánsdóttir, S. (2013). *Microseismicity in the Krýsuvík Geothermal Field, SW Iceland, from May to October 2009*. Master thesis, University of Iceland.

Lawver, L. and Müller, R. (1994). Iceland hotspot track. *Geology*, 22(April 1994):311–314.

Ljunggren, C., Chang, Y., Janson, T., and Christiansson, R. (2003). An overview of rock stress measurement methods. *International Journal of Rock Mechanics and Mining Sciences*, 40(7-8):975–989.

Lund, B. and Bödvarsson, R. (2002). Correlation of Microearthquake Body-Wave Spectral Amplitudes. *Bulletin of the Seismological Society of America*, 92(6):2419–2433.

Lund, B. and Slunga, R. (1999). Stress tensor inversion using detailed microearthquake information and stability constraints: Application to ölfus in southwest Iceland. *Journal of Geophysical Research*, 104(B7):14947.

Mardia, K. (1972). *Statistics of Directional Data: Probability and Mathematical Statistics*. Academic Press, London.

Martínez-Garzón, P., Bohnhoff, M., Kwiatek, G., and Dresen, G. (2013). Stress tensor changes related to fluid injection at The Geysers geothermal field, California. *Geophysical Research Letters*, 40(11):2596–2601.

Mastin, L. (1988). Effect of borehole deviation on breakout orientations. *Journal of Geophysical Research*, 93(B8):9187.

McDougall, I., Kristjánsson, L., and Sæmundsson, K. (1984). Magnetostratigraphy and geochronology of northwest Iceland. *Journal of Geophysical Research*, 89(B8):7029–7060.

McKenzie, D. (1969). The relation between fault plane solutions for earthquakes and the directions of the principal stresses. *Bulletin of the Seismological Society of America*, 59(2):591–601.

Moorbath, S., Sigurdsson, H., and Goodwin, R. (1968). K-Ar ages of the oldest exposed rocks in Iceland. *Earth and Planetary Science Letters*, 4(3):197–205.

Müller, B., Zoback, M., and Fuchs, K. (1992). Regional patterns of tectonic stress in Europe. *Journal of Geophysical Research : Solid Earth*, 97(B8):11783–11803.

Nakamura, K. (1977). Volcanoes as possible indicators of tectonic stress orientation - principle and proposal. *Journal of Volcanology and Geothermal Research*, 2:1–16.

Nettles, M. and Ekström, G. (1998). Faulting mechanism of anomalous earthquakes near Bárðarbunga Volcano, Iceland. *Journal of Geophysical Research*, 103(B8):17973–17983.

Peška, P. and Zoback, M. D. (1995). Compressive and tensile failure of inclined well bores and determination of in situ stress and rock strength. *Journal of Geophysical Research*, 100(B7):12791.

Pierdominici, S. and Heidbach, O. (2012). Stress field of Italy - Mean stress orientation at different depths and wave-length of the stress pattern. *Tectonophysics*, 532-535:301–311.

Plateaux, R., Bergerat, F., Béthoux, N., Villemin, T., and Gerbault, M. (2012). Implications of fracturing mechanisms and fluid pressure on earthquakes and fault slip data in the east Iceland rift zone. *Tectonophysics*, 581:19–34.

Plateaux, R., Béthoux, N., Bergerat, F., and Mercier de Lépinay, B. (2014). Volcano-tectonic interactions revealed by inversion of focal mechanisms: stress field insight around and beneath the Vatnajökull ice cap in Iceland. *Frontiers in Earth Science*, 2(May):1–21.

Ragnarsson, Á. (2015). Geothermal Development in Iceland 2010-2014. In *Proceedings World Geothermal Congress 2015*, volume 2010, page 15, Melbourne.

Rajabi, M., Tingay, M., King, R., and Heidbach, O. (2016). Present-day stress orientation in the Clarence-Moreton Basin of New South Wales, Australia: A new high density dataset reveals local stress rotations. *Basin Research*.

Reasenberg, P. A. and Simpson, R. W. (1992). Response of regional seismicity to the static stress change produced by the Ioma Prieta earthquake. *Science*, 255(5052):1687–1690.

Reinecker, J., Tingay, M., Müller, B., and Heidbach, O. (2010). Present-day stress orientation in the Molasse Basin. *Tectonophysics*, 482(1-4):129–138.

Reiter, K. and Heidbach, O. (2014). 3-D geomechanical-numerical model of the contemporary crustal stress state in the Alberta Basin (Canada). *Solid Earth*, 5(2):1123–1149.

Reiter, K., Heidbach, O., Schmitt, D., Haug, K., Ziegler, M., and Moeck, I. (2014). A revised crustal stress orientation database for Canada. *Tectonophysics*, 636:111–124.

Richardson, R. M. (1992). Ridge forces, absolute plate motions, and the intraplate stress field. *Journal of Geophysical Research*, 97(B8):11739.

Röckel, T. and Lempp, C. (2003). Der Spannungszustand im Norddeutschen Becken. *Erdöl Erdgas Kohle*, 119(2):73–80.

Rögnvaldsson, S. and Slunga, R. (1994). Single and joint fault plane solutions for microearthquakes in South Iceland. *Tectonophysics*, 237:73–80.

Roman, D. C., Moran, S., Power, J., and Cashman, K. (2004). Temporal and Spatial Variation of Local Stress Fields before and after the 1992 Eruptions of Crater Peak Vent, Mount Spurr Volcano, Alaska. *Bulletin of the Seismological Society of America*, 94(6):2366–2379.

Roth, F. and Fleckenstein, P. (2001). Stress orientations found in north-east Germany differ from the West European trend. *Terra Nova*, 13(4):289–296.

Roth, F., Henneberg, K., Fleckenstein, P., Palmer, J., Stefanssson, V., and Gudlaugsson, S. (2000). Ergebnisse von Bohrloch-Spannungsmessungen in der Südisländischen Seismizitätszone. *Mitteilungen / Deutsche Geophysikalische Gesellschaft*, 3:49–50.

Sæmundsson, K. (1974). Evolution of the axial rifting zone in northern Iceland and the Tjörnes fracture zone. *Geological Society of America Bulletin*, 85(4):495–504.

Sæmundsson, K. (1978). Fissure swarms and central volcanoes of the neovolcanic zones of Iceland. *Geol. J. Spec*, 10:415–432.

Sæmundsson, K. (1979). Outline of the geology of Iceland. *Jökull*, 29:7–28.

Sæmundsson, K. (1986). Subaerial volcanism in the western North Atlantic. *The Geology of North America*, 1000:69–86.

Sánchez, J. J., Wyss, M., and R. McNutt, S. (2004). Temporal-spatial variations of stress at Redoubt volcano, Alaska, inferred from inversion of fault plane solutions. *Journal of Volcanology and Geothermal Research*, 130(1-2):1–30.

Sbar, M. L. and Sykes, L. R. (1973). Contemporary compressive stress and seismicity in eastern North America: an example of intra-plate tectonics. *Geological Society of America Bulletin*, 84(6):1861–1882.

Schäfer, K. and Keil, S. (1979). In situ Gesteinsspannungsermittlungen in Island. *Messtechnische Briefe*, 15(2):35–46.

Scheidegger, A. (1962). Stresses in the earth's crust as determined from hydraulic fracturing data. *Geologie und Bauwesen*, 27(2):1.

Segall, P. and Fitzgerald, S. D. (1998). A note on induced stress changes in hydrocarbon and geothermal reservoirs. *Tectonophysics*, 289(1-3):117–128.

Sigmundsson, F., Einarsson, P., Halldorson, P., Jakobsdottir, S., Vogfjörd, K., Sigbjörnsson, R., and Snaebjörnsson, J. T. (2005). Earthquakes and faults in the Kárahnjúkar area. Technical Report March, Jardvisindastofnun Haskolans.

Sigmundsson, F., Hooper, A., Hreinsdóttir, S., Vogfjörd, K. S., Ófeigsson, B. G., Heimisson, E. R., Dumont, S., Parks, M., Spaans, K., Gudmundsson, G. B., Drouin, V., Árnadóttir, T., Jónsdóttir, K., Gudmundsson, M. T., Högnadóttir, T., Fridriksdóttir, H. M., Hensch, M., Einarsson, P., Magnússon, E., Samsonov, S., Brandsdóttir, B., White, R. S., Ágústsdóttir, T., Greenfield, T., Green, R. G., Hjartardóttir, Á. R., Pedersen, R., Bennett, R. A., Geirsson, H., La Femina, P. C., Björnsson, H., Pálsson, F., Sturkell, E., Bean, C. J., Möllhoff, M., Braiden, A. K., and Eibl, E. P. S. (2015). Segmented lateral dyke growth in a rifting event at Bardarbunga volcanic system, Iceland. *Nature*, 517(7533):191–5.

Sigurdsson, H. (1970). Structural origin and plate tectonics of the Snaefellsnes volcanic zone, Western Iceland. *Earth and Planetary Science Letters*, 10(1):129–135.

Sigurdsson, H. and Sparks, R. S. J. (1978). Rifting episode in North Iceland in 1874 - 1875 and the eruptions of Askja and Sveinagja. *Bulletin Volcanologique*, 41(3):149–167.

Sinton, J., Grönvold, K., and Sæmundsson, K. (2005). Postglacial eruptive history of the Western Volcanic Zone, Iceland. *Geochemistry, Geophysics, Geosystems*, 6(12):n/a–n/a.

Soosalu, H. and Einarsson, P. (1997). Seismicity around the Hekla and Torfajökull volcanoes, Iceland, during a volcanically quiet period, 1991-1995. *Bulletin of Volcanology*, 59(1):36–48.

Sperner, B., Muller, B., Heidbach, O., Delvaux, D., Reinecker, J., and Fuchs, K. (2003). Tectonic stress in the Earth's crust: advances in the World Stress Map project. *Geological Society, London, Special Publications*, 212(1):101–116.

Stefánsson, R. (1966). Methods of focal mechanism studies with application to two Atlantic earthquakes. *Tectonophysics*, 3(3):209–243.

Stefánsson, R., Gudmundsson, G. B., and Halldórsson, P. (2000). The two large earthquakes in the South Iceland seismie zone on June 17 and 21, 2000. Technical Report July, Icelandic Meterological Organisation, Reykjavík.

Stefánsson, R., Gudmundsson, G. B., and Halldorsson, P. (2008). Tjörnes fracture zone. New and old seismic evidences for the link between the North Iceland rift zone and the Mid-Atlantic ridge. *Tectonophysics*, 447(1):117–126.

Sykes, L. and Sbar, M. (1974). Focal mechanism solutions of intraplate earthquakes and stresses in the lithosphere. In Kristjansson, L., editor, *Geodynamics of Iceland and the North Atlantic Area*, pages 207–224. D. Reidel Publishing Company, Dordrecht-Holland.

Sykes, L. R. (1967). Mechanism of earthquakes and nature of faulting on the mid-oceanic ridges. *Journal of Geophysical Research*, 72(8):2131–2153.

Thordarson, T. and Larsen, G. (2007). Volcanism in Iceland in historical time: Volcano types, eruption styles and eruptive history. *Journal of Geodynamics*, 43(1):118–152.

Tibaldi, A., Bonali, F. L., Pasquaré, F. A., Rust, D., Cavallo, A., and D'Urso, A. (2013). Structure of regional dykes and local cone sheets in the Midhyrna-Lysuskard area, Snaefellsnes Peninsula (NW Iceland). *Bulletin of Volcanology*, 75(11):764.

Tingay, M., Müller, B., Reinecker, J., Heidbach, O., Wenzel, F., and Fleckenstein, P. (2005). Understanding tectonic stress in the oil patch: The World Stress Map Project. *The Leading Edge*, 24(12):1276–1282.

Villemin, T., Bergerat, F., Angelier, J., and Lacasse, C. (1994). Brittle deformation and fracture patterns on oceanic rift shoulders: the Esja peninsula, SW Iceland. *Journal of Structural Geology*, 16(12):1641–1654.

Ward, P. (1971). New interpretation of the geology of Iceland. *Geological Society of America Bulletin*, 82(11):2991–3012.

Wessel, P., Smith, W. H. F., Scharroo, R., Luis, J., and Wobbe, F. (2013). Generic Mapping Tools: Improved Version Released. *Eos, Transactions American Geophysical Union*, 94(45):409–410.

White, R. S., Drew, J., Martens, H. R., Key, J., Soosalu, H., and Jakobsdóttir, S. S. (2011). Dynamics of dyke intrusion in the mid-crust of Iceland. *Earth and Planetary Science Letters*, 304(3):300–312.

Wiens, D. A. and Stein, S. (1984). Intraplate seismicity and stresses in young oceanic lithosphere. *Journal of Geophysical Research*, 89(B13):11442.

Wiprut, D., Zoback, M., Hanssen, T., and Peska, P. (1997). Constraining the full stress tensor from observations of drilling-induced tensile fractures and leak-off tests: application to borehole stability and sand production on the. *International Journal of Rock Mechanics and Mining Sciences*, 34(365):3–4.

Wolfe, C. J., Th. Bjarnason, I., VanDecar, J. C., and Solomon, S. C. (1997). Seismic structure of the Iceland mantle plume. *Nature*, 385(6613):245–247.

Zang, A. and Stephansson, O. (2010). *Stress Field of the Earth's Crust*. Springer Netherlands, Dordrecht.

Zoback, M. and Zoback, M. (1991). Tectonic stress field of North America and relative plate motions. In Slemmons, D. and Engdahl, E., editors, *Neotectonics of North America*, pages 339–366. Geological Society of America, Boulder, Colorado.

Zoback, M. L. (1992). First- and second-order patterns of stress in the lithosphere: The World Stress Map Project. *Journal of Geophysical Research*, 97(B8):11703.

Zoback, M. L., Zoback, M. D., Adams, J., Assumpção, M., Bell, S., Bergman, E. A., Blümling, P., Brereton, N. R., Denham, D., Ding, J., Fuchs, K., Gay, N., Gregersen, S., Gupta, H. K., Gvishiani, A., Jacob, K., Klein, R., Knoll, P., Magee, M., Mercier, J. L., Müller, B. C., Paquin, C., Rajendran, K., Stephansson, O., Suarez, G., Suter, M., Udias, A., Xu, Z. H., and Zhizhin, M. (1989). Global patterns of tectonic stress. *Nature*, 341(6240):291–298.